DOUBLE-SKIN SYSTEM OF ROOM-SIDE AIR GAP APPLIED TO DETACHED HOUSE (PART 1): SIMULATION ANALYSIS FOR REDUCTION OF COOLING LOAD IN THE FORCED VENTILATED WALL OF DETACHED HOUSE

Kan Lin[1], Shinsuke Kato[*2], Togo Yoshidomi[3], and Kyosuke Hiyama[4]

1 Graduate School of The University of Tokyo
7-3-1, Hongo, Bunkyo-ku,
Tokyo, Japan

2 IIS, The University of Tokyo
4-6-1 Komaba, Meguro-Ku,
Tokyo, Japan
**Corresponding author: kato@iis.u-tokyo.ac.jp*

3 Graduate School of The University of Tokyo
7-3-1, Hongo, Bunkyo-ku,
Tokyo, Japan

4 Yamaguchi University
1677-1, Yoshida, Yamaguchi-shi,
Yamaguchi, Japan

ABSTRACT

Detached residential wooden houses are a common type of housing in Japan. Decay of wooden components within the walls caused by condensation or defective flushing, is sometimes an issue. To solve this problem, a double-skin system with a room-side air gap was developed. In this system, during summer, the airflow that is driven by ventilation fans moves through the room-side air gap in the wall, and removes heat load either from the inner surface of the insulation material, or from the surface adjacent to the rooms inside. The purpose of this study is to evaluate the flow rate in the ventilated wall, controlled by ventilation fans. The airflow in the ventilated wall removes heat from the surface of the wall and influences occupants' thermal comfort. Therefore, it is important to develop an expression for flow rate in the wall. An airflow-energy simulation program was used to predict flow rates in the ventilated wall, and the performance of air-flows in several exterior walls of the house was investigated under various conditions. The results verify that the flow rate in the ventilated walls increased with the ventilation fan speed. By using forced ventilation, the cooling load was reduced by 10% to 20%.

KEYWORDS

Double-skin system, Detached house, Simulation, Forced ventilation, Cooling load

1 INTRODUCTION

Wooden detached houses, which have wood-based structural insulation materials for walls and flooring, are widely used in Japan. However, many problems exist with this type of home construction. For example, during the summer period, incoming solar radiation is not equally distributed, leading to uneven indoor temperature distribution. In the winter period, indoor humidity is closely related to the durability of the building envelope. Moisture leaking from the interior rooms increases the risk of condensation on the walls, because the surface temperature of the wall is low. Condensation on the walls may cause the wood used in the houses' construction to decay. In addition to condensation from interior rooms, water vapour condenses on wooden window frames, and rainwater can leak through the roof and walls. The increased moisture is absorbed by the wooden structure of the house, and reduces the endurance and strength of the wood, and also accelerates its decay.

To remove the moisture between the external and internal walls, a double-skin system is commonly installed to detached houses. A double-skin system consists of a multi-layered façade, with a buffer space used for ventilation. Air flow in the ventilated wall is controlled by ventilation fans set atop the roof. This system can integrate the mechanical ventilation with natural ventilation so that air can move freely in the buffer space.

In summer, air vents in the basement are opened and the ventilation fans on top of the roof are turned on to facilitate airflow through the ventilated wall, and out the roof. Airflow in the ventilated wall removes heat from solar radiation and from the internal wall. The airflow discharges heat in the wall and attic space, while obtaining cold heat from the ground under the floor. This ensures that the rooms are kept in moderate temperature and comfort.

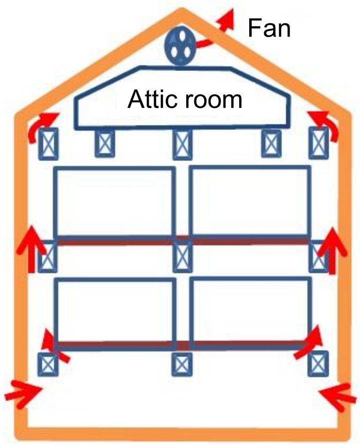

Figure 1: Double-skin system of room-side air gap with ventilated wall applied to detached house

Although houses using this system have been built for about 30 years in Japan, only a few studies have been conducted on them. Using a simulation of a model house from previous research, Ozaki et al. analyzed the airflow speed in the wall, as well as the airflow in the space under the floor during the summer period. However, there is hardly any information available regarding the actual airflow and thermal effects of this system. For this reason, it is difficult to select appropriate strategies to maintain airflow rate in the ventilated wall.

The objective of this study is to understand the basic properties of the double-skin system, temperature drop, and reduction in cooling load during the summer period by performing a ventilation network simulation. To perform calculations during the summer period, we used a network simulation by creating two building models with spaces in the air gap and rooms of the house that were regarded as independent nodes. The impact of each element to the airflow rate was estimated, and the cooling load reduction effect of the system was examined in the simulation.

The results show the relationship between different patterns of the airflow rate and reduction in the cooling load. The reduction in the cooling load increased with the flow rate of the ventilation fans. In addition, natural indoor temperature drop effects became more significant with the increase in the flow rate of the ventilation fans.

2 MATERIALS AND METHODS

2.1 Simulation Software

To calculate the airflow in the buffer space, we used the variable energy calculation software TRNSYS17, and its add-on program TRNFlow. TRNFlow is designed based on COMIS3.1, a ventilation network calculation software, and can perform the iterative calculations by resolving the movement of the air and heat at the same time in TRNSYS.

2.2 Building Model

In this research, the house model (4th region) proposed by IBEC, Institute for Building Environment and Energy Conservation, as a standard detached house in Japan was used in the simulation. This house model is a two-story house with 120.07 m^2 total floor area, and it is intended for a four-person family. There are several spaces divided by rooms, as shown in figure 2. Occupants' schedules as well as the lighting, equipment, ventilation, and air conditioning are based on the investigation. The dimensions and the basic configuration of the building were set based on this model. In addition, the dimensions of the air gap in the ventilated wall were set based on the real house.

The air gap in the ventilated wall is shown in figure 3. The area of the air gap in which air moves upwards is represented as the blue portion. Grooves are arranged on the surface of the insulation material in equal intervals. These create openings between the insulation and the other components, so that air flows freely. The air gap is divided into several zones by resistance parts, such as vents or these openings. In such zones, the flow path is narrower than the open air gap. For the calculations by TRNFlow, we modeled the air gap as an “airnode,” and defined any resistance parts as an “airlink.” For each airlink, the relationship of the mass flow rate and the pressure difference is calculated based on equation (1). In equation (1), a common formula for ventilation, the value of $C_{s,}$ for each airlink, was decided by fixing α to 0.6 as a typical value. Also determined was the opening area A of the airlink, from the actual specification of this house. The value of n was determined to be 0.5, from the above substitution for the opening area, which is reflected in equation (2).

$$\dot{m} = C_s \cdot (\Delta p)^n \tag{1}$$

$$\dot{m} = \alpha A \sqrt{2\rho \cdot \Delta p} \tag{2}$$

$\dot{m}$: Δp mass flow rate [kg / h], α: pressure difference [Pa], C_s: flow coefficient [-],
A: opening area [m^2], ρ: air density [kg/m^3]

In this simulation, a simple building model that does not take into account the air infiltration, was used; neither air leaking into the rooms, nor outside air from the gas passage is considered. A simple network that connects the air gap to the outside air was created, as shown in figure 4.

With this model, it is possible to estimate the potential of the maximum amount of airflow generated by mechanical ventilation, regardless of the influence of air infiltration. On the other hand, because heat from solar radiation and internal heat cannot be discharged by infiltration, simulation results may show that the room temperature is higher than the actual environment.

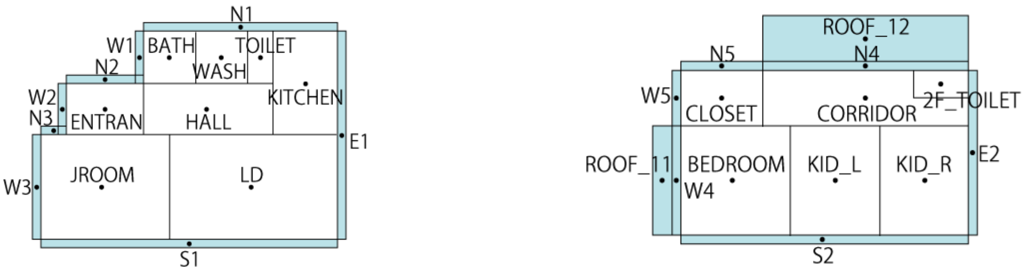

Figure 2: Zones and airnodes of the building model in TRNSYS

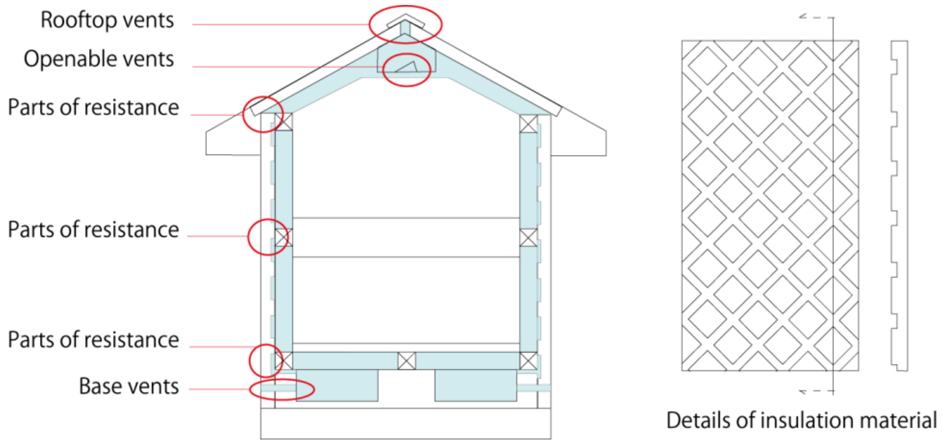

Figure 3: Overview of the air gap and insulation material

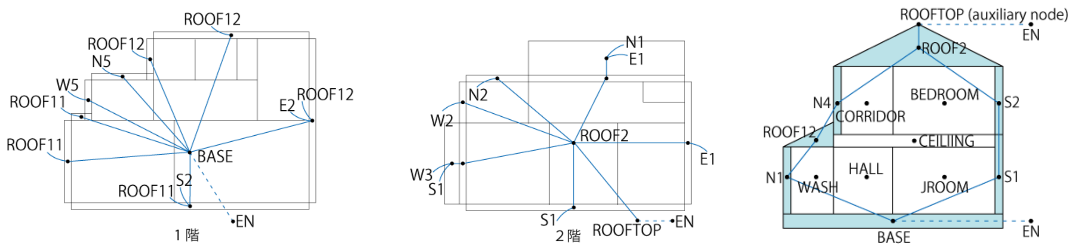

Figure 4 : Overview of airlinks in TRNFlow

Table 1: Building Properties

Wall of external side	Extruded polystyrene foam = 50 mm + Air layer = 15 mm + Tile = 10 mm
Wall of internal side	Gypsum board = 13 mm
Air gap thickness	120 mm
Roof	Extruded polystyrene foam = 50 mm + Air layer = 30 mm + Plywood = 10 mm + Slate = 5 mm
Base	EPS 50 mm + RC 150 mm + EPS 50 mm
Internal wall, Ceiling, Floor	U = 3.125 W/m^{2}K, 4.082 W/m^{2}K, 4.082 W/m^{2}K
Window, double-glazing	U = 1.8 W/m^{2}K, Shading coefficient = 0.5
Infiltration	None

Table 2: Ventilated Wall Setting

Opening area A [m^2]	Part of resistance in the air gap	0.00396 m^2/m (opening area per unit length wall)
	Ventilation unit at the rooftop to outside	0.0919
	Attic space to the ventilation unit at the rooftop	0.0755
	Outside to under-floor space	0.0720
Constants		α = 0.6, ρ = 1.2, n = 0.5

Table 3: Calculation Conditions

Internal heat gain	Exists (based on the schedule by IBEC)
Ventilation	None
Air-conditioning	None, Exists (based on the schedule by IBEC)
Surface temperature in the under-floor space	20°C
Weather data	Expanded AMeDAS standard data (2000) , Tokyo
External wind	None
Calculation period	7/21–8/20, 6/1–9/30 (plus 3 days for run-up period)

Table 4: Simulation Cases

	Flow rate of the attic fan (m^3/h)	**Multiplier (-)**
Case 0	0 (off)	-
Case 1	150	1/2

Case 2	300	1
Case 3	600	2

2.3 Calculation Conditions

The calculation conditions used in this study are listed in Table 1 through Table 4. Table 1 lists the properties of the walls, air gap, windows, etc. The conditions of the ventilated wall are listed in Table 2, and the calculation conditions are listed in Table 3. For evaluating the airflow rate, four cases under different flow rates are supposed. To estimate effects under different airflow rates, the flow rate of the basic case (Case 0) is set to 0 m^3/h, and the main flow rate is set to 300 m^3/h (Case 2). Other cases are multiplied by 0.5 or 2, respectively. The simulation cases are listed in Table 4.

To estimate the properties of airflow in the ventilated wall at natural room temperature, the simulation was first performed without air-conditioning. Then, calculations were carried out with air conditioning, and the effect of cooling load reduction due to heat loss carried by airflow in the wall was estimated. The air-conditioning temperature was set to 28°C, and a total of five rooms—living room, kitchen, bedroom, and two children's rooms—were regarded as air-conditioned.

As shown in Table 3, the schedule of internal heat generation, ventilation, and air-conditioning was set according to the criteria of the IBEC standard. The ground surface temperature of the subfloor space was set to 20°C, in reference to the results of past measurements. For weather data, including external wind, AMeDAS' expansion 2000 standard data in Tokyo was used. The calculation period was 7/21–8/20 (plus 3 days for run-up period) in the study of airflow rate, and was 6/1–9/30 (plus 3 days for run-up period) in the study of the cooling load reduction effect.

3 RESULTS

The average flow rate for each wall is shown in Figure 5. The bars with black frames represent the second floor, and the bars without black frames represent the ground floor. The figure shows positive airflow in all walls, and flow direction along a wall (upward direction) is considered positive. For the case in which the flow rate is 300 m^3/h, the average velocity is 54.0 cm/s on the first floor and 66.9 cm/s on the second floor. When the flow rate changes from 300 m^3/h to 150 m^3/h and then to 600 m^3/h, the average flow rate in this period changes by a factor of 0.5 and 2, respectively.

Figure 6 shows the results of a natural indoor temperature and the temperature decrease for Case 2, in which the airflow rate is 300 m^3/h. The temperature in the living room drops by 1.5–3.5°C. The temperature in the roof changes drastically, and the biggest drop is as much as 4.8°C. Also, the average indoor temperature decline is about 2.6°C over the same period.

Figure 7 shows the flow rate of each wall during the representative days, by direction. Based on the graph, the flow rate for each wall is affected by the outdoor temperature. The flow rates in the walls N1, N3, W1, and W3 are low when compared to the other walls, which range from 45 to 50 cm/s.

Figure 8 shows the temperature decreasing in six airnodes. The effect of the temperature decrease in each room is especially remarkable. However, the temperature of the base airnode rises when the flow rate of the ventilated walls is increased. When outdoor air goes through the base airnode, outdoor air is cooled and the base airnode obtains heat from the outdoor air. The largest temperature decrease, 5.4°C, appears on the airnode of roof2, which is at the top of the house. Over a period of time, a decrease of 2.0°C in the indoor temperature can be achieved when the flow rate is 150 m^3/h; 2.6°C, when it is 300 m^3/h; and 4.7°C, when it is 600 m^3/h.

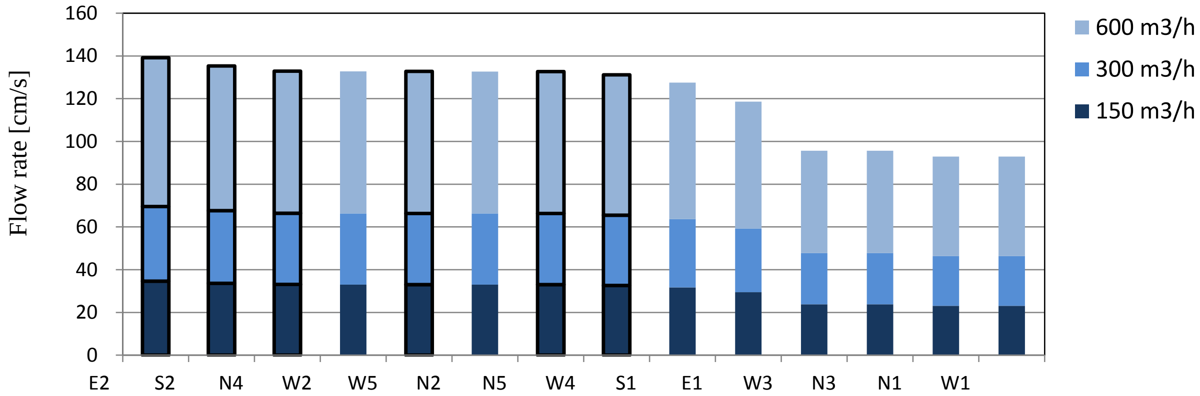

Figure 5: Average flow rate of each wall

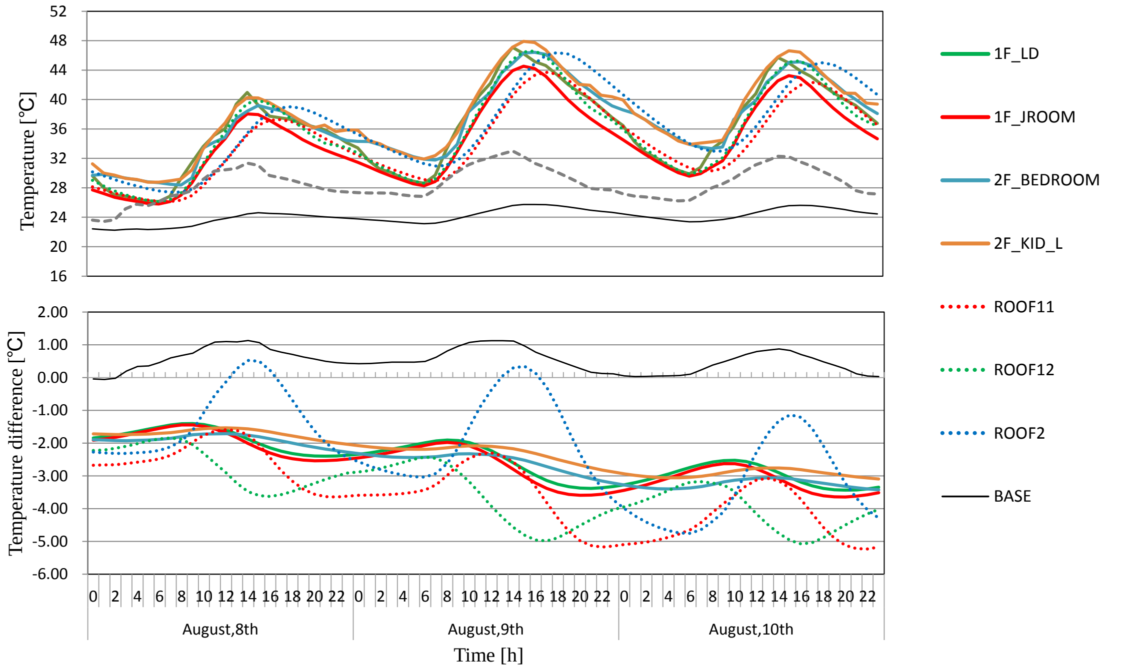

Figure 6: Temperature decrease during representative days (Case 2, 300 m^3/h)

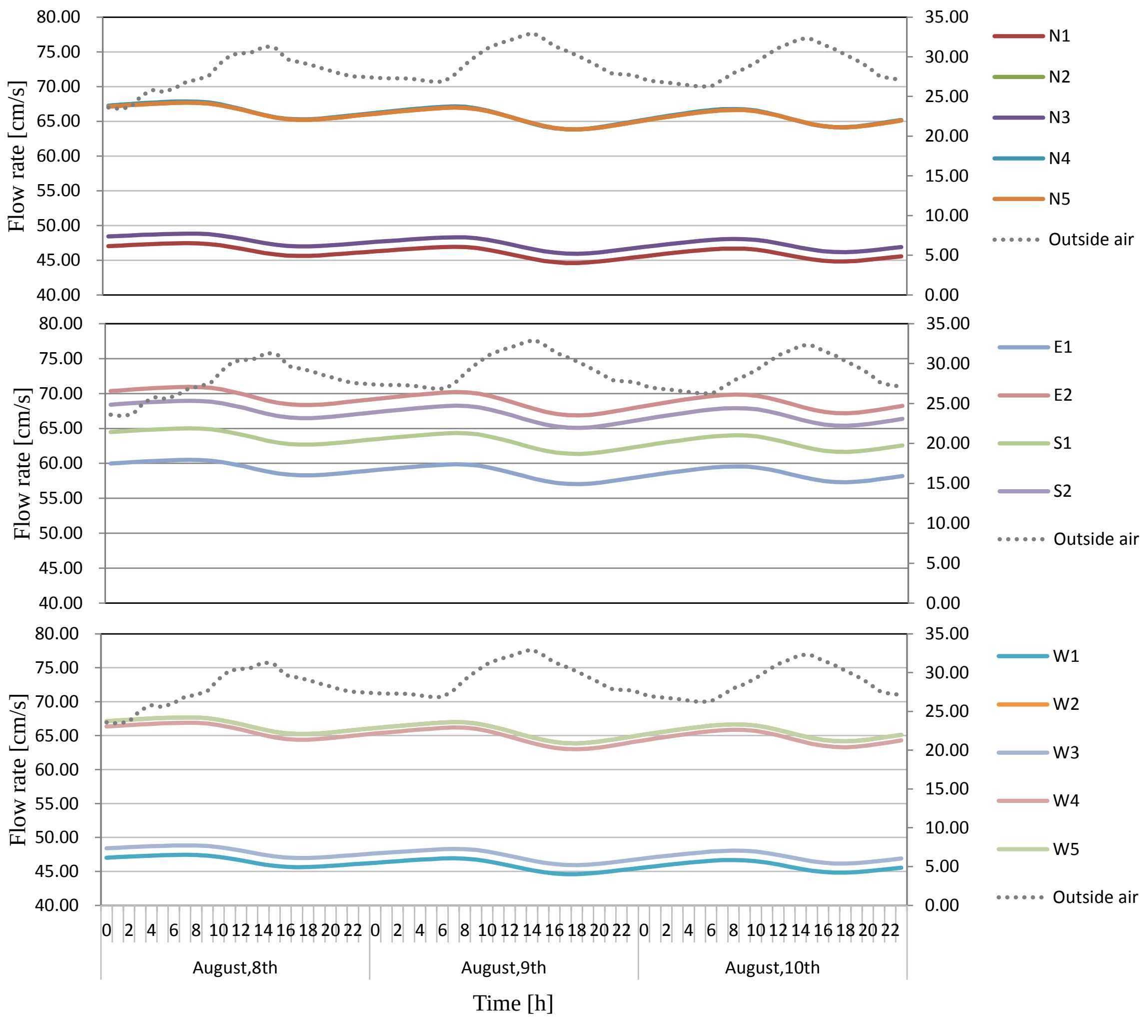

Figure 7: Flow rate for each wall during representative days (Case 2, 300 m^3/h)

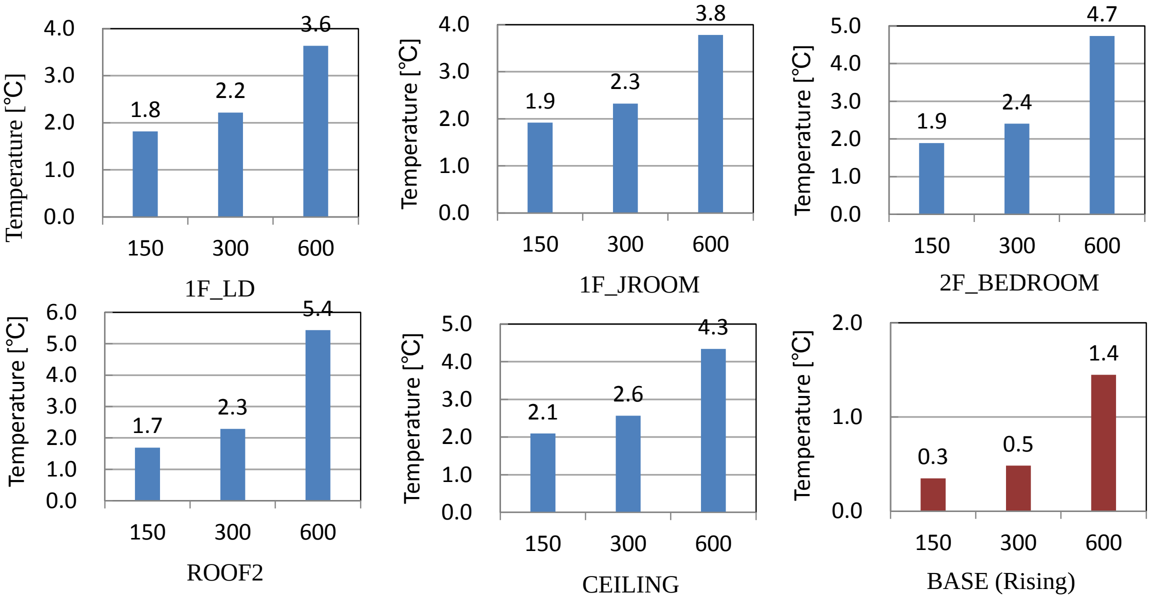

Figure 8: Temperature Decreasing in Each Airnode

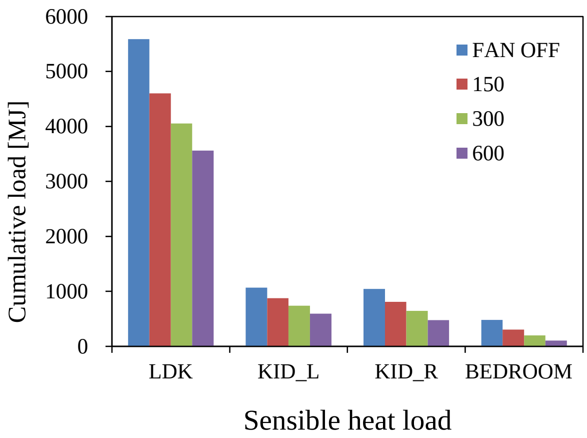

Figure 9: Total cooling load in each room

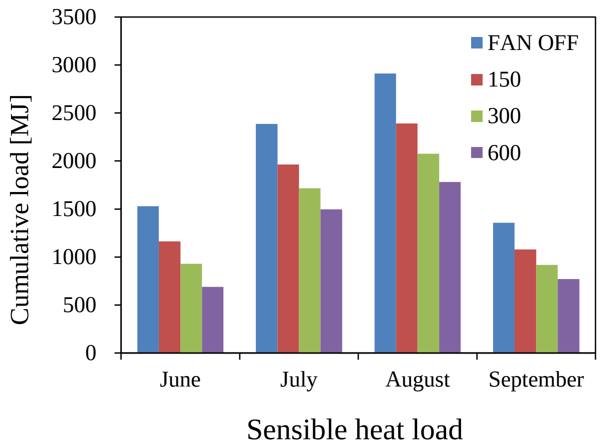

Figure 10: Total cooling load in each month

Figure 9 shows the total cooling load in the ventilated walls for each room and flow rate, for the case with air-conditioning set at 28°C. Results for the four rooms are shown in the graph. The dining room (LDK) receives the largest cooling load reduction because it consumes the most energy among the four rooms. The average cooling load reduction for the dining room from June to September was reduced by 27%.

Figure 10 shows the total cooling load from June to September for each month. The cooling load was reduced for the cases with flow rates equal to 150 m^3/h, 300 m^3/h and 600 m^3/h, and the average cooling load during the period from June to September was reduced by 19%, 31%, and 42%, respectively. The reduction was largest in June and September in which the temperature was lowest. The cooling load was reduced by 28% for a flow rate of 300 m^3/h, even in August, which is the hottest month.

4 CONCLUSIONS

In this study, we evaluated the airflow rate in the air gap of a double-skin cooling system, the cooling load reduction, and the temperature decrease by performing a ventilation network simulation. When changing the airflow of the fan, cooling is improved as the ventilation quantity increases. If the flow rate changes by a factor of 0.5 and 2, the average flow along the wall changes by a factor of 0.5 and 2, respectively. In general, the cooling effect is greater when the flow rate is higher. Over a period of time, a decrease in 2.0°C in the indoor temperature can be achieved when the flow rate is 150 m^3/h; 2.6°C, when it is 300 m^3/h; and 4.7°C, when it is 600 m^3/h, respectively. The cooling load was reduced for the cases with flow rates of 150 m^3/h, 300 m^3/h, and 600 m^3/h, and the average cooling load during the period from June to September was reduced by 19%, 31%, and 42%, respectively. Reduction was largest in June and September, when the temperatures were the lowest. The cooling load was reduced by 28% for a ventilated flow rate of 300 m^3/h, even in August, which is the hottest month.

It was found that the total period cooling load is reduced while the ventilated wall is working and the air-conditioning is on. It seems that this effect is mainly because the air-conditioning settling time was reduced by the room temperature drops. As a result, it is expected that the cooling load reduction effect is dependent on the flow rate of the ventilated wall and the cooling load supplied from subfloor ground surface Therefore, a further simulation of geothermal heat is necessary for future study. Furthermore, because heat from solar radiation and internal heat cannot be discharged by infiltration, the simulation result shows the the room temperature is higher than that of the actual environment. To evaluate the influence of infiltration, a simulation that considers infiltration between the interior-exterior wall interface and between the wall-room interface is needed in further research.

5 REFERENCES

Ozaki, A. (1992). Heat and water transfer through an ventilated structure using urethane panels [in Japanese]. *Summaries of technical papers of Annual Meeting Architectural Institute of Japan, D,* 945-946.

Institute for Building Environment and Energy Conservation. (2009). *Description of the energy consumption calculation method in the standards of judgment of the housing business building owners* [in Japanese].

Kurabuchi, T. (2009). Wind tunnel experiments on surface wind pressure and cross-ventilation flow rate in densely populated residential area: study on proper design method of locating windows aiming at utilization of cross-ventilation in densely populated residential area (part 1) [in Japanese]. *Journal of environmental engineering 74(642), 951-956*.